LA-5084-MS

INFORMAL REPORT

Magnetic Measurements on the LASL Prototype Magnet

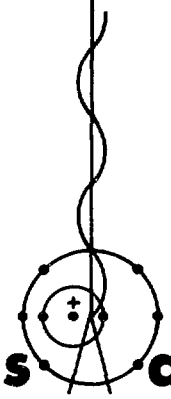

los alamos
scientific laboratory
of the University of California
LOS ALAMOS, NEW MEXICO 87544

UNITED STATES
ATOMIC ENERGY COMMISSION
CONTRACT W-7405-ENG. 36

In the interest of prompt distribution, this LAMS report was not edited by the Technical Information staff.

Printed in the United States of America. Available from
National Technical Information Service
U. S. Department of Commerce
5285 Port Royal Road
Springfield, Virginia 22151
Price: Printed Copy $3.00; Microfiche $0.95

LA-5084-MS
Informal Report
UC-28
ISSUED: November 1972

los alamos
scientific laboratory
of the University of California
LOS ALAMOS, NEW MEXICO 87544

Magnetic Measurements on the LASL Prototype Magnet*

by

W. Dunwoody
R. Rolfe**
J. Spencer
R. Stearns†
N. Tanaka
M. Thomason††

*Presented at the 4th International Magnet Conference, Battelle Northwest Laboratories, Richmond, WA, September 1972.

**Permanent address: Physics Department, University of California, Los Angeles, CA 90024.

†Permanent address: Physics Department, Vassar College, Poughkeepsie, NY 12601.

††Permanent address: Physics Department, University of Virginia, Charlottesville, VA 22901.

Sponsored by Associated Western Universities.

MAGNETIC MEASUREMENTS ON THE LASL PROTOTYPE MAGNET

by

W. Dunwoody, R. Rolfe, J. Spencer,
R. Stearns, N. Tanaka, and M. Thomason

ABSTRACT

A small dipole magnet has been designed and constructed for use as a prototype for the kinds of magnets to be used with the High Resolving Power Spectrometer (HRS) and the Energetic Pion Channel and Spectrometer (EPICS) facilities currently under construction at the Los Alamos Scientific Laboratory. Because of the wide range in uniform field strengths and the high degree of homogeneity which is required in these magnets, a more versatile method than pole face shims or homogenizers was considered necessary. A set of corrective current elements, called H_t-windings, were introduced inside the pole pieces of the magnet to provide dynamic correction of field inhomogeneities in the uniform field region. By successively varying these currents and plotting the resulting field distribution, $B_y(x)$, it was possible to reduce magnetic field variations of a few parts in 10^3 in the initial median plane distribution to a few parts in 10^5 over a range of induction fields of B_o = 4-17 kG. These initial results indicate that field homogeneities significantly better than 1 part in 10^5 should be possible with the appropriate number and distribution of H_t-current elements.

I. INTRODUCTION

For spectrometers where resolving powers as high as 10^5 are desired, such as in the HRS system, it is necessary to obtain homogeneous magnetic fields of 1 part in 10^5 or better. In the past a variety of methods have been used to obtain field homogeneities on the order of one part in 10^4 or so, but these appear impractical when one wants to achieve an order of magnitude improvement and at the same time maintain this level for a significant range of field strengths. One method which seems desirable is to have a number of free parameters which can be adjusted to counter the effects of varying pole face distortions and saturation of the iron with changing field level as well as other changes in the magnetic properties of the iron which might arise during the fabrication process or later. Results presented here indicate that the H_t-windings[1] and their associated currents represent a viable set of parameters for such purposes. An additional advantage of this particular choice is that it also provides us the possibility of introducing second, third, and higher order moments in the field distribution should the beam optics require it.

The primary purpose for constructing the prototype magnet was to study the effectiveness of the H_t-windings as well as a number of other features which were built into it such as field clamps with adjustable nosepieces, removable pole tips, contoured pole edges and an homogenizing slot running along one edge parallel to the beam direction. This last characteristic was added to explore the effect of the pole edge contour on the useful magnetic width of the magnet. Several different types of measurements were performed to assess the influence of such elements on the overall field distribution. A list of these and other related measurements which were done, including certain mechanical and thermal tests, are given below:

1. x,z scans of the uniform field, $B_y(x,z)$ from $B_o \simeq 4 - 17$ kG,
2. Effective field length of the magnet vs x and B_o,
3. Fringe field distributions at the square and circular ends,

4. Effective field length as a function of field clamp position,
5. Flux measurements in various parts of the field clamps,
6. Measurements of certain rate-dependent effects,
7. Influence of H_t currents on the central field distribution,
8. Adjustment of H_t currents via computer optimization,
9. Measurement of temperature gradients during operation, and
10. Measurement of gap distortions due to thermal gradients, etc.

Because of space limitations and the fact that the H_t-windings may be of more specific interest we have decided to confine our discussion here primarily to items 7 and 8 together with the overall description of the prototype magnet and how the H_t-windings have been incorporated into its design.

II. DESCRIPTION OF THE DESIGN

In order to adequately simulate the EPICS and HRS bending magnets, the prototype was designed to be operated with one of the HRS power supplies (current stability of better than 10^{-5} over most of its range) with saddle coils capable of producing fields of approximately 20 kG. The physical dimensions of the prototype are one-third to one-fifth those of the full scale magnets. The steel which was used had a carbon content ranging from ASA-1006 to 1010. The pole pieces were made from 2-in.-thick ASA-1008 steel which was ultrasonically tested in accordance with ASTM-A-435. The following additional constraints were made: 1) that the scanning grid should be continuous and include 100% coverage and 2) that the rejection standard should be any discontinuity exceeding 50% loss of back reflection using a 1-in.-diam transducer.

The overall layout of the prototype is shown in Fig. 1 together with our convention for the coordinate system which has been used. Figure 2 is a schematic top-view including the adjustable nosepieces on both the square and circular boundaries of the magnet. Along one of the edges perpendicular to the square entrance boundary, the edge is contoured in the same way as the two HRS dipoles. The other edge has the "homogenizing" slot mentioned above. This is 75 mils in width and runs the length of the magnet with a depth equal to the pole piece thickness which is 1-1/2 in. Because of the presence of this slot, the outside H_t slot was eliminated on this side of the magnet. As a result, the total number of H_t current elements in the prototype is seven rather than eight as on the EPICS and HRS magnets and they are spaced at intervals of 3-in. from one another which in this particular case corresponds to one gap height.

Figure 3 is a cross sectional view with the lower half taken through one of the H_t current slots to show the H_t current path through the iron. The field clamps and the extended nose pieces are shown,

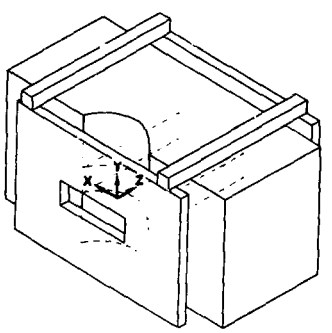

Fig. 1. Isometric layout of the prototype magnet with the coordinate system which has been used here.

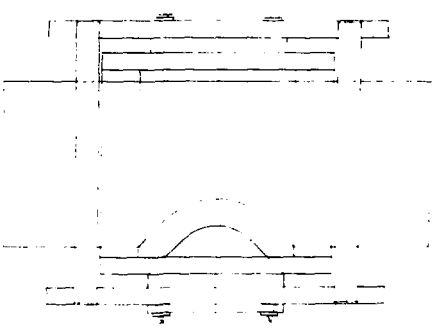

Fig. 2. Top view of the prototype showing the yoke, coil, and field clamps with their nosepiece extensions.

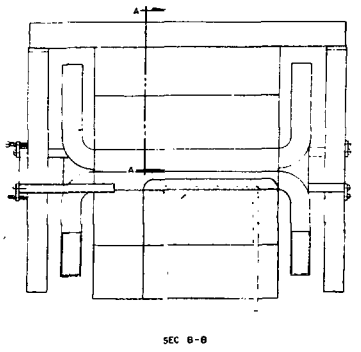

Fig. 3. Cross section view of the prototype showing the paddle-coils, nosepiece extensions, and a cut through an H_t-winding slot.

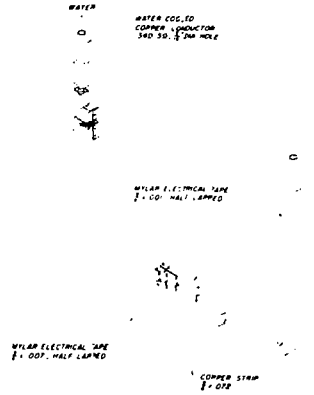

Fig. 4. Detail of an H_t-winding as used in the prototype.

together with the saddle coil which was used. This coil follows the contour of the iron except in the vicinity of the circular pole boundary.

III. H_t-WINDINGS FOR THE PROTOTYPE

One of the more imporant features of the prototype was the H_t current configuration. This part of the overall design was developed in close accord with Halbach's theory.[1] Since the H_t-windings of the prototype are very short, the voltage across each power supply is very small. Operation under this kind of condition could cause instability in the power supply. This problem can be overcome by adding a series resistor in the circuit or lengthening the conductor by having multiple turns on the H_t-windings. Consequently it was decided that the H_t-windings on the prototype magnet would be multiturn like those planned for the EPICS magnets.

The arrangement of the conductors is shown in Fig. 4. Each H_t-winding consists of one water-cooled conductor of 0.340-in.-sq. x 0.1835-in. i.d. and four 3/8-in. x 0.072-in. copper strips. The four strips are arranged such that they are cooled by the water-cooled conductor. Series connections of these conductors were made outside of the yoke by using heavy copper bars. Since the potential difference between any two conductors is small, half-lapped 1.0-mil-thick mylar electrical tape was sufficient insulation. Ground plane insulation consists of half-lapped 7-mil-thick electrical tape. Before and after each H_t-winding assembly was placed in the yoke of the magnet, hi-pot tests of 500 V were performed between every two conductor combination and also between ground and each conductor.

IV. INITIAL PERFORMANCE CHARACTERISTICS

A magnetization curve for the prototype was measured and is shown in Fig. 5 with the expected results. As one can see from Fig. 6, one of the first transverse field scans across the median plane taken well inside the magnet showed a quite nonuniform distribution with a slight depression of approximately 1 - 2 in. in width corresponding to a field perturbation of about 1 part in 3000. This bump extended the full length of the magnet parallel to the central axis. It was learned that during the grinding process on the pole face the pole piece had to be reoriented in order to machine the entire surface. This procedure caused a small section of the pole surface near the center and along the entire length to receive extra grinding. This introduced a

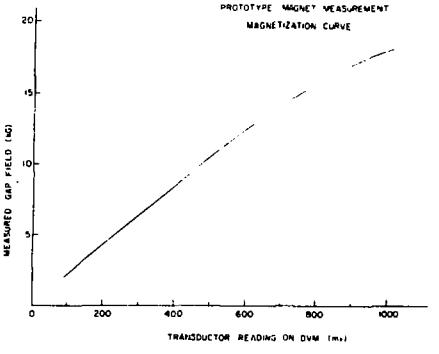

Fig. 5. Magnetication curve for the prototype.

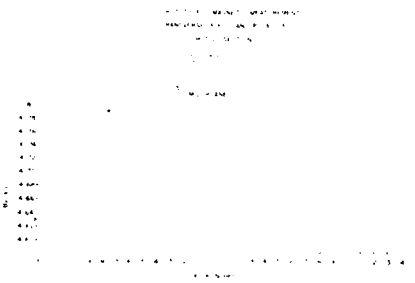

Fig. 6. An initial transverse median plane field distribution shown relative to the prototype pole configuration. The homogenizing slot is shown on the right.

discontinuity on each pole face of approximately 0.5 mil. This effect was present on both pole faces at approximately the same location, thus the total gap variation was on the order of 1.0 mil. Since the width of field variation resulting from the above is smaller than the spacings of the H_t-windings, it is impossible to correct such an effect with the windings used here. In order to eliminate this bump the two pole pieces were reground without reorientation. After reassembly, field measurement showed that this had eliminated the bump in the field distribution.

V. H_t-WINDING MEASUREMENTS

The objective of the first set of H_t-winding measurements was to obtain the best possible field uniformity by means of manual adjustment of the currents in the different windings. A block diagram of the equipment which was used is shown in Fig. 7. A small flux coil 0.464-in. in diameter and 0.330-in. high was used as a probe. The coil was wound with 3886 turns of number 40 wire. Measurements such as shown in Fig. 6 were made by moving this coil along the transverse direction. The signal induced in the coil by the variation of the field along the path was fed into an integrator whose output was displayed on a DVM (H.P. #2401C). The field variations seen during a sweep were plotted on an x-y recorder (H.P. #7005B) by displaying the integrator signal on the y-coordinate and the transverse position of the coil on the x-coordinate. The calibration for these measurements was obtained by moving the coil from a position in the field clamp

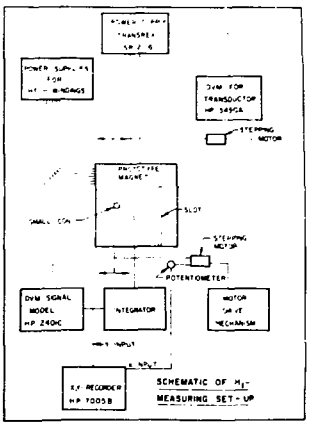

Fig. 7. Block diagram of the equipment used in the initial H_t-winding measurements.

where the field was assumed to be zero into a region of the magnet where the field was known from NMR measurements.

The measurements were begun by sweeping the field with no currents in the H_t-windings. Each winding was then turned on separately to observe its effect on the field. These data were then used to estimate the best current changes to be made. Successive adjustments of the currents were then made until satisfactory results were obtained. This procedure was followed successfully at field levels of 3.7, 14.5, and 17.3 kG.

A second objective was to measure the field uniformity as a function of the z-coordinate once the homogeneity had been optimized at the central position. Without changing the H_t-currents, coil sweeps were made at three inches closer to the curved end of the magnet and at three inches closer to the straight end of the magnet. The results of this manual optimization at 3.7 kG are shown in Fig. 8.

These results should be compared with those at a similar field level shown in Fig. 6 above. Although the results of this study definitely demonstrate the capabilities of the H_t-windings, the method of adjusting the current is time consuming and too cumbersome to be useful in applications requiring frequent adjustments. Since our application involves situations where there may be frequent changes in the field level, a computer optimization procedure was developed.

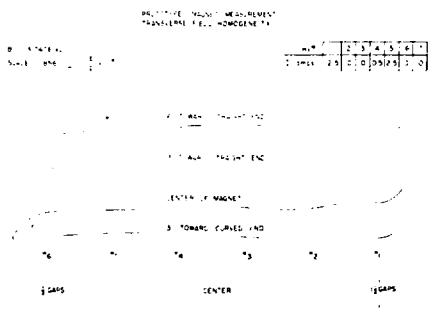

Fig. 8. First results of manually adjusting the H_t-windings at 3.7 kG. The numbers at the bottom represent the locations of the H_t elements.

VI. H_t TUNING PROCEDURE AND RESULTS

To accomplish the computer optimization of the H_t currents, we have used a weighted, least squares procedure to extract the optimum current values. Figure 9 shows the kind of data which is input for the program. The basic procedure employed was to set the different H_t currents at some starting values (possibly all zero) and then to take the magnet to saturation. The field was then reduced slowly to the desired value and allowed to remain there for about 10 minutes, after which an x-scan was made and recorded. Each H_t current was then varied independently of the rest by approximately ± 20 amperes and after each current setting was made the magnet was again returned to saturation and brought back to the desired field value according to the above procedure before the corresponding field scan was carried out. Since the field was always measured at the same value of x (≡0) on coming down from saturation, the distribution for x = 0 is always a horizontal line in Fig. 9 while the other curves vary smoothly with the current. By making the measurements with an NMR probe these curves are generally reproducible to about 1 part in 10^5. This procedure yielded the necessary partial derivatives needed for the optimization. The results were then fed into the computer which predicted a new set of H_t currents and the whole procedure repeated.

Figure 10 shows a typical result of optimizing the x-distribution for a fixed value of z. Two iterations of the procedure just outlined were required to obtain this particular result. The measured results follow the predicted trend quite closely considering the fact that the measurements were not analyzed with an on-line computer. This generally resulted in a delay of a full day between successive iterations.

Having obtained an adequate distribution at one value of z it was of interest to look at other z-values without reoptimizing. Figure 11 shows some of the results. Since the distributions tend to get worse as one moves away from the location where the optimization was performed it is clear that the optimization should be done by obtaining several x-scans at different values of z. This would be necessary unless one knew that the x-distribution remains unchanged as a function of z or else can optimize a single x-scan considerably better than the average distribution required throughout the magnet. Figure 12 shows our first results of including two different z locations in the H_t optimization.

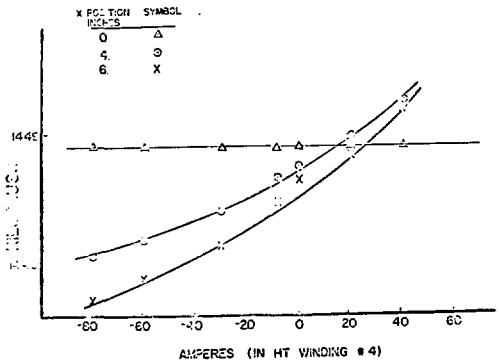

Fig. 9. Effect of energizing H_t current #4 on the transverse field distribution.

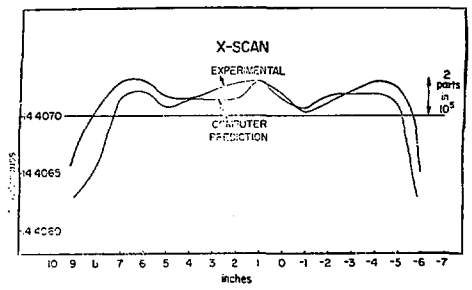

Fig. 10. Comparison between the computer prediction and the observed transverse field distribution. The field is uniform to better than two parts in 10^5 over a range of four gap widths in x.

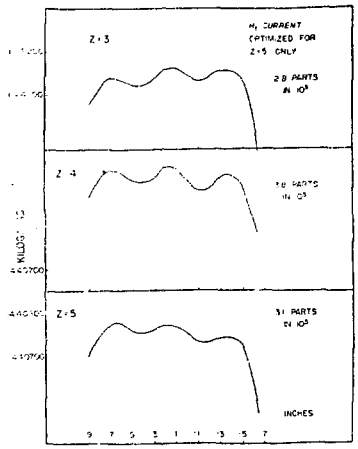

Fig. 11. Typical results as a function of z-value when the x-distribution is optimized at only one value of z.

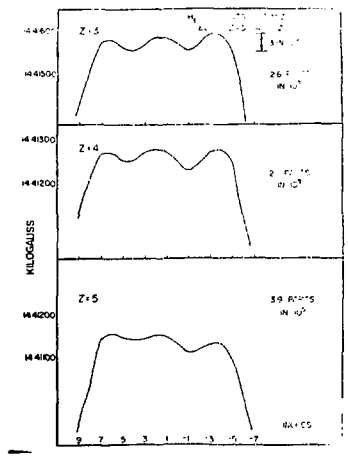

Fig. 12. Results of optimizing the x-distribution at two different z-values simultaneously.

Since the H_t-windings run parallel to z, any variation of the x-distribution with z can only be improved in an average way unless the variation is a systematic one such as a uniform increase in field level with z but with no corresponding change in the shape of the x-distribution. In any case, the correct procedure for optimizing at several values of z is to consider each one independently with its own values of $B_y(x=0)$ and partial derivatives. This was not done in the case shown in Fig. 12 and this may account for the undramatic improvement, even though there are variations in the shape of the x-scans. H_t currents cannot correct these variations unless there are independent sets of them placed successively along the z-direction. The number of such sets as well as the number and distribution of H_t currents perpendicular to the z-direction determine the ultimate homogeneity one can hope to obtain in any configuration. In the HRS, the dipoles have three independent sets spaced successively along the pole length (total length = 180 in.) with eight independent windings per set spaced across the pole width (total width between outer elements = 28 in.).

Of course, when one is working with parts in 10^5 there are any number of additional factors which could limit these results such as inaccuracies in the measurements or the optimization, all of which become increasingly important as one approaches the desired solution. To minimize the significance of short term instabilities, the measurements should be carried out and analyzed as quickly as possible since it is virtually impossible to filter all of the noise sources in an experimental area. In the HRS system there will be one remotely-controlled NMR probe per set of eight H_t currents. Their outputs will be read directly by the computer so that the optimization procedure will be completely automated. This should also allow for more efficient operational use of the spectrometer since angular distributions will require frequent changes in the base field level.

Although extensive measurements were not made, we did explore how small changes in the central field level influenced the uniformity of the x-scans following optimization. For a field uniformity on the order of 2.5 parts in 10^5 the field may be increased or decreased by about 0.1 kG without changing the uniformity of the x-scan appreciably. A change of 0.2 kG produced a nonuniformity of about 6.6 parts in 10^5 while a change of 0.5 kG resulted in more than 3 parts in 10^4. There was also evidence that it is better to make a slight decrease rather than an increase when a change is necessary. This is consistent with hysteresis considerations and fortunately accords with how one normally obtains experimental angular distributions.

It was also found, as might be expected, that one cannot return to the original central field value for which the x-scan was optimized and still expect it to be as uniform. In returning to the original central field setting after a decrease of

about 0.34 kG, the nonuniformity had increased to something on the order of 9 or 10 parts in 10^5.

On the other hand, stopping at a higher central field value on the way down from saturation appears to be of little help in improving the results of the optimization. For a central field optimized at 14.4 kG a nonuniformity of 9 parts in 10^5 was found when a scan was made at 14.6 kG on the way down from saturation while the uniformity was still about 2.5 in 10^5 on returning to 14.4 kG.

From all of the above, it is clear that when frequent field changes are necessary an efficient optimization procedure is needed. For a system such as the HRS, it would be nice to have the computer scan the three NMR probes in any one magnet simultaneously while it is analyzing the scan results from another magnet. Beyond the question of time this is because it may prove necessary to optimize the magnet as a whole rather than optimizing successive H_t sets along z. Unfortunately, one question we could not explore with the prototype magnet was how successive sets of H_t-windings interact with one another. Insofar as any single current element is concerned, however, it is clear from the measurements that its effect is not localized to its immediate vicinity but generally extends across the width of the pole.

VII. RATE-DEPENDENT LIMITATIONS

To insure generally reproducible results with the H_t-windings it appears necessary to make frequent traversals of the main hysteresis loop of the magnet (or at least a portion of it) in order to eliminate remanent effects of one H_t-winding on the corresponding results for the others. Although this can be a time consuming procedure, it will also fail if the field changes are not carried out slowly enough. We have observed at least two effects when the main field is quickly reduced from saturation to the desired lower value. First the central field at some particular x value will slowly drift to lower values and secondly the uniformity of a particular x-distribution is worsened. These effects were measured by bringing the central field from saturation to about 14.4 kG in times of 12 sec, 120 sec, 5 min. and 10 min. The results are shown in Figs. 13 through 15. The upper curves show how the field drifted after the initial decrease from saturation. The lower curves show the corresponding x-distribution

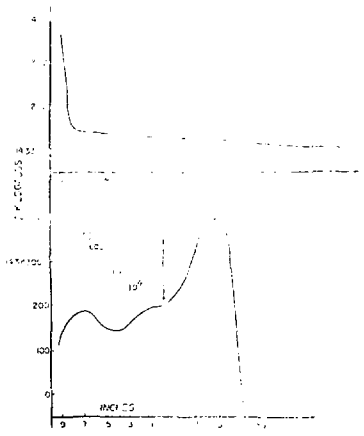

Fig. 13. Results of reducing the central field from full saturation to 14.3 kG in 12 sec.

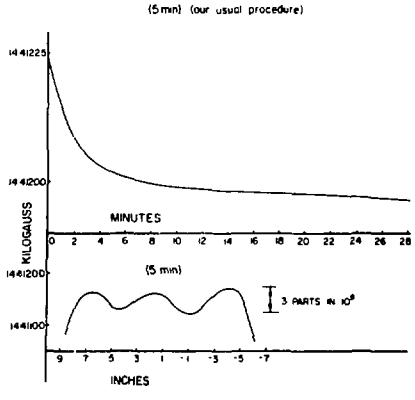

Fig. 14. Corresponding results for 5 min.

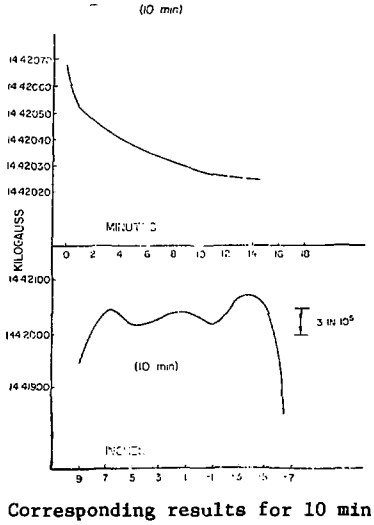

Fig. 15. Corresponding results for 10 min. The lower curve shows results taken 20 min. after the field reduction.

after a measured settling period. This period was 20 min. except for the shortest time which was about 30 min.

Typically, the field drift is about 0.3 gauss in the first 15 min., for reduction times of about 4 min. or more with a gradual drift thereafter which can amount to a gauss or so in 24 hr. The influence on the x-distribution for times on the order of 2 min. or less is significant at the levels of field uniformity considered here, although at lower levels it does not seem particularly significant. For example, without energizing the H_t currents such variations are generally negligible compared with the other variations observed in the distribution. The largest variations which were observed in this regard always occurred on the side without the slot, i.e., the slot improved the homogeneity of the magnet. We understand that similar variations as we observed here in the x-direction have also been observed in the z-direction.[2]

The first effect mentioned above is probably dominated by the time constant of the overall system while the second is due to the induced eddy currents which will be highest at the edges of the iron nearest the coils. For systems where field variations along the z-direction can be detrimental, as with the H_t-windings, we conclude that saddle coils or their equivalent should be used depending on the level of field inhomogeneity which can be tolerated.

VIII. OTHER MEASUREMENTS

In order to study the usefulness for high resolving power of other features, such as the field clamps, we performed a series of different measurements of the effective length. The initial results, for a given field clamp position, were generally greater than those expected from the design calculations obtained using the two-dimensional code POISSON. In constrast, the measured fringing field distribution along the axis agrees quite well with the calculations. Since the discrepancy in the effective length increased with increasing central field value, at least part of the difference was due to saturation of certain parts of the field clamp. Since this effect becomes apparent at rather low fields, it can become a significant problem for high resolving power systems which have to operate over an extended range of central field values. As a result, a series of flux measurements were made in the field clamp to determine the specific regions of saturation. These and other measurements are described below.

One important conclusion is that for a properly contoured pole edge it should be possible to design a field clamp and nosepiece extension which give an effective length which is stable to about 10 mils or better over a range of central field values from 4-17 kG. Since this statement continues to be valid for a range of distances of the field clamp or, more importantly, the nosepiece from the magnet, one would have a simple, inexpensive means of inducing, within certain limits, higher order curvatures on the effective field boundary of a magnet or of modifying or correcting an existing curvature.

A. Effective Length

The prototype magnet has been used to study the behavior of the effective length, ℓ_{eff}, as a function of varying field level and for different field clamp configurations. The measurements were made with an $\int Bd\ell$ coil by feeding the coil signal directly into a DVM. The coil had 60 turns of number 36 wire with a length = 96.25 in. and width = 0.895 in. The physical arrangement allowed measurements along the central axis (x,y=0) as well as for different transverse locations in the median plane.

The value of ℓ_{eff} calculated with the POISSON-Code[3] was 22.22 in. with the field clamp extensions both located 4.5 in. from the magnet. This is shown in Fig. 16 together with measurements of the effective length vs transverse position in the magnet at two different fields. Part of the discrepancy here may

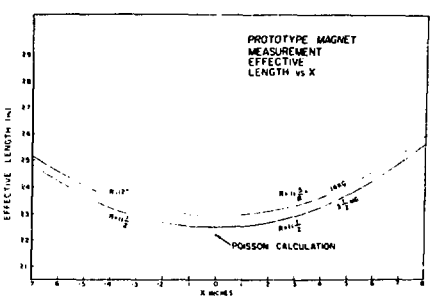

Fig. 16. Effective length vs transverse position, x, at 3.5 and 14 kG. The prototype is not a magnetically symmetric system because of the homogenizing slot at x = 10-3/4-in.

be due to the fact that the saddle coil is square while the pole is circular so that the two-dimensional field calculation has to be corrected. This specific coil configuration also makes saturation of the nosepiece on the circular end more likely. Since the difference in the POISSON predictions for the two different fields was small compared to what was observed and since the divergence between the predicted and observed results increases with central field value, it was suspected that the observed spread was very likely due to saturation of the nosepiece or certain parts of the clamp or perhaps both.

Figures 17 and 18 show plots of ℓ_{eff} vs the central induction field for different positions of the nosepieces. All measurements were made along the central axis of the magnet with the field clamps at a fixed distance from the magnet. The arrows on the curves indicate the direction by which the field was approached. The discrepancy between the results for the two directions is largest at the lowest fields -- the two curves only converging in the vicinity of 20 kG. In all cases, the effective length is larger when going up in field than when returning from saturation.

In Fig. 17 the nosepiece at the curved end was pulled well out from the magnet to insure that it would not saturate, in order to study effects at the straight end. When going up in field, the varaation of ℓ_{eff} with B_o is about 50 mils or less over the range from 4 - 17 kG and is always less than when returning from saturation. In either case, however, the effective elngth varies less than 10 mils as a function of nosepiece position for a total motion of the nosepiece from about 2-1/2 gaps out to within 1-1/2 gaps from the magnet. Over this range of positions the location of the effective field boundary varied from approximately 0.09 in. per 1-in. movement of the nosepiece to 0.18 in. per 1-in. change of the nosepiece, respectively.

The corresponding results at the curved end are shown in Fig. 18. In general, the motion of the effective field boundary is larger here per unit change of the nosepiece than at the straight boundary being about 0.15 in. per 1-in. movement of the nosepiece at 2-1/2 gaps from the magnet. Also the change of the effective length with field is generally larger here but both of these effects may be due to the onset of saturation which is evident from the trend of the data as the nosepiece is moved inward. Although a small change in ℓ_{eff} is expected from the calculations at the higher field levels, the lower curve indicates nearly a one-half-in. change which is more than an order of magnitude greater than predicted using POISSON. These results showed that saturation was occurring somewhere in the field clamp at the curved end.

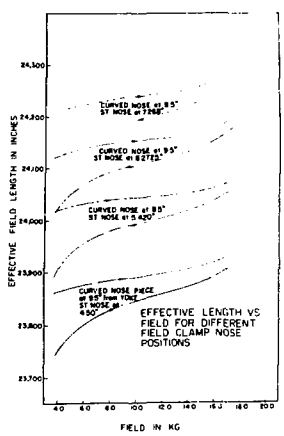

Fig. 17. Effective length along the symmetry axis (x,y=0) vs the central induction field for the nosepiece at the curved end fixed at 9.5 in. from the yoke.

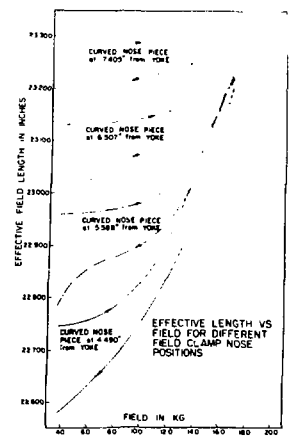

Fig. 18. Effective length along the symmetry axis vs the central induction field from 3.8 - 16.8 kG for four different locations of the curved nosepiece.

B. Flux Measurements in the Field Clamp

The study of the effective length as a function of field strength and field clamp position led to the belief that certain sections of the field clamp might be saturating. It was decided to investigate four positions in the field clamp on the curved end of the magnet. These positions are shown in Fig. 19:

1. 3-3/16-in. from the tip of the field clamp nose,
2. 7-3/4-in. from the tip of the field clamp nose,
3. The support-leg for the nosepiece, and
4. The return-leg of the main field clamp.

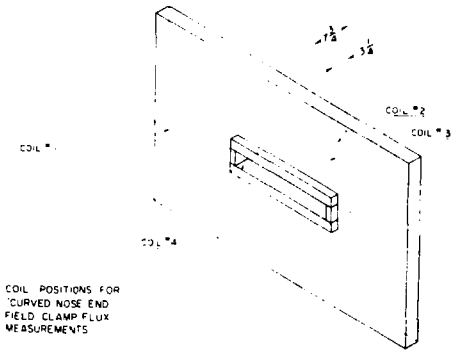

Fig. 19. Locations of flux measurements in the field clamp and nosepiece at the circular end of the prototype.

Calibration was performed by using a rectangular coil of 18-1/4-in. x 3-in. This coil was placed in the uniform field region of the magnet and the field was increased in steps from zero to 16.8 kG. The signal from the coil was read by a DVM through the integrator. These data gave a calibration curve.

The measurements of the field in the various places in the field clamp were then carried out by winding a coil around the position in question. This coil had the same number of turns as the calbration coil. The same procedure was followed as for the calibration, that is, the field was raised from zero to the desired field levels in the magnet gap and the signals from the coil were read by the DVM through the integrator. The fields were then calculated using the formula

$$\text{(field in desired position)} = \frac{VA_o}{V_o A} = B_o$$

where

A_o = cross sectional area of calibration coil

V_o = DVM output from the calibration coil

V = DVM output from the coil in the desired position

A = cross sectional area of the coil

B_o = field measured in the gap by means of a Hall probe.

Very briefly, the results illustrated in Fig. 20 are:

1. The field in the nosepiece at 3-3/16 in. from the tip of the field clamp varies from 4 kG at a gap field of 3.8 kG to 16.4 kG at a gap field of 16.8 kG.
2. The field in the nosepiece at 7-3/4 in. from the tip of the field clamp varies from 5 kG at a gap field of 3.8 kG to 18.8 kG at a gap field of 16.8 kG.
3. The field in the support-leg of the nosepiece varies from 8 kG at a gap field of 3.8 kG to 23.2 kG at a gap field of 16.8 kG.
4. The field in the return-leg of the main field clamp varies from 1 kG at a gap field of 3.8 kG to 5.7 kG at a gap field of 16.8 kG.

They show that the worst saturation occurs in the support-leg of the nosepiece. Further study

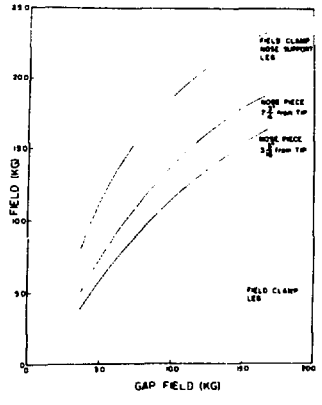

Fig. 20. Average fields obtained from the flux measurements made at the four locations shown in Fig. 19.

will be conducted here with nosepieces of increased thickness and better quality of iron.

The results presented here are representative of the measurements we have made on the prototype magnet. Analysis of much of these results is still in progress as are a number of additional measurements which have been suggested by some of this work. In particular, we hope to improve the H_t analysis procedure to provide field uniformities better than 1 part in 10^5 which is the level which will be required by the High Resolving Power Spectrometer system at LAMPF.

IX. ACKNOWLEDGMENTS

The authors would like to thank Drs. K. Halbach, W. V. Hassenzahl, and H. A. Thiessen for their various contributions to this work. In particular, the idea for the homogenizing slot as well as the H_t-windings is due to K. Halbach who was also instrumental in our initiating the eddy current measurements. They also wish to thank Cecil Stark for his help in the preparation of the manuscript.

References

1. Klaus Halbach, Lawrence Berekeley Laboratory Report, UCRL-18969 (1971).

2. Karl Brown, private communication.

3. Ron Yourd, private communication.